

Quadruple Anionic Buckybowls by Solid-State Chemistry of Corannulene and Cesium

Tobias Bauert,[†] Laura Zoppi,[‡] Georg Koller,[§] Jay S. Siegel,[‡] Kim K. Baldridge,^{*,‡} and Karl-Heinz Ernst^{*,†,‡}

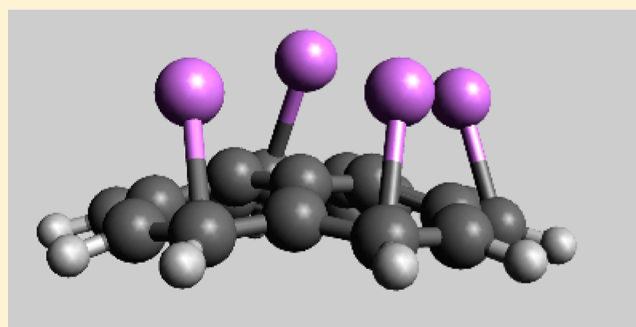
[†]Empa, Swiss Federal Laboratories for Materials Science and Technology, Überlandstrasse 129, CH-8600 Dübendorf, Switzerland

[‡]Department of Chemistry, University Zurich, CH-8057 Zürich, Switzerland

[§]Institut für Physik, Karl-Franzens-Universität Graz, Universitätsplatz 5, 8010 Graz, Austria

Supporting Information

ABSTRACT: The buckybowl corannulene is known to be an excellent electron acceptor. UV photoelectron spectroscopy studies were performed with thin-film systems containing corannulene and cesium. Adsorption of submonolayer quantities of corannulene in ultrahigh vacuum onto thick Cs films, deposited at 100 K on a copper(111) substrate, induces a transfer of four electrons per molecule into the two lowest unoccupied orbitals. Annealing of thick corannulene layers on top of the cesium film leads to the formation of a stable film composed of $C_{20}H_{10}^{4-}$ ions coordinated to four Cs^+ ions. First-principles calculations reveal, as the most stable configuration, four Cs^+ ions sandwiched between two corannulene bowls.



INTRODUCTION

Large efforts to identify organic superconductors with a high superconducting transition temperature (T_c) have been undertaken but with limited success so far.¹ Graphite-intercalation superconductors, such as KC_8 , CaC_6 , and YbC_6 with T_c typically in the range of 0.5–12 K were described early on.^{2–4} With the advent of C_{60} in the 1990s came alkali-metal doping of fcc- C_{60} crystals which led to T_c as high as 38 K.^{5,6} In this decade, the alkali-metal doped planar aromatic hydrocarbon (PAH) picene was found to become superconducting at 18 K,⁷ and very recently potassium doped “few-layer graphene material” showed a transition temperature of 4.5 K.⁸ A very promising candidate for alkali-doped organic superconductivity is corannulene (**1**, $C_{20}H_{10}$, Figure 1), a bowl-shaped PAH fragment of C_{60} . Transition temperatures of up to 66 K for the monoanion of **1** have been predicted by theoretical modeling of intermolecular electron–phonon coupling.⁹

Motivated by the novel bowl-shape and five-fold symmetry of **1**, studies of corannulene-coated metal surfaces have revealed

numerous surface stereochemical principles, such as optimal packing strategies of five-fold symmetric molecules in the plane,^{10,11} effects of symmetry mismatch between substrate and molecules,^{12–14} 2D phase transitions,^{15,16} bicomponent packing,¹⁷ and surface-induced ball- and bowl-in-bowl complexation.^{18,19} These primarily structural studies allow one to develop a molecular-based materials chemistry for **1**.

Having a π -electronic surface area comparable to that of pyrene or perilene,^{20,21} **1** should also display exceptional photophysical and electrochemical properties as a material,²² such as the intense blue-light electroluminescence reported for **1**,²³ and the particularly intriguing, large electron-acceptor ability of **1**, which, if normalized per carbon atom, goes beyond that of C_{60} .²⁴ C_{60} , with a triply degenerate lowest unoccupied molecular orbital (LUMO), can accommodate six extra electrons over 60 carbon atoms ($0.1 e^-/C$ atom), whereas corannulene with a doubly degenerate LUMO can accommodate four extra electrons ($0.5 e^-/C$ atom). Seminal work characterized tetralithium-**1** complexes in solution,²⁵ but it stays unresolved that **1** cannot form a $C_{20}H_{10}^{4-}$ anion with larger ions, such as potassium.²⁶ In particular, it has been suggested that alkali-**1** complexes of the type $X_4C_{20}H_{10}$ ($X \neq Li$) will not form sandwich structures with four alkali ions located between two bowl molecules, as was the case for Li_4 -**1**.²⁷ Until recently,²⁸ compounds containing anions of **1** were exclusively characterized in solution, and there only the tetraanionic Li -**1** aggregate has been identified.²⁹ Such tetraanionic Li -**1** motif has

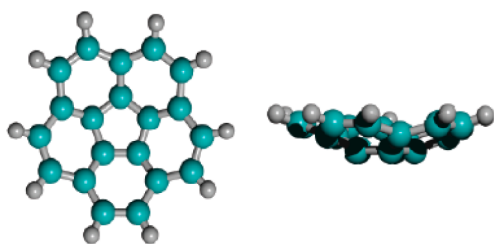


Figure 1. Ball-and-stick model of corannulene, $C_{20}H_{10}$.

Received: June 22, 2013

Published: July 27, 2013

also been used to create supramolecular architectures with bicorannulenyli.³⁰

In refutation of the current hypothesis, this study shows that codeposition of **1** and Cs metal onto a Cu(111) surface under ultrahigh vacuum (UHV) conditions leads to a **1**-Cs₄ compound with a structure analogous to the Li₄C₂₀H₁₀ complex. UV photoelectron spectra clearly reveal charge transfer from Cs to **1** and the occupation of the two degenerate LUMOs. Theoretical calculations suggest four Cs ions between two distorted bowls of **1** are aligned in a square and a complete occupation of the two lowest unoccupied orbitals, LUMO and LUMO+1.

METHODS SECTION

Experimental Section. The experiments were performed in an UHV chamber ($p < 2 \times 10^{-10}$ mbar), equipped with standard surface science techniques like X-ray photoelectron spectroscopy (XPS), UV photoelectron spectroscopy (UPS), low-energy electron diffraction (LEED), and thermal desorption spectroscopy (TDS). After synthesis and purification of **1**,²⁰ thermal evaporation ($T_{\text{cell}} = 384$ K) was performed from an effusion cell. Cesium was evaporated by using a dispenser (SAES), which contained Cs₂CrO₄ embedded in Al and Zr, acting as an oxygen getter. They are stable in air and easy to handle. The copper(111) surface (Matek, Germany) was cleaned and prepared *in vacuo* by repeated cycles of Ar-ion sputtering and annealing at 800 K.³¹ The cleanliness and surface crystallinity was checked by XPS and LEED. A monolayer of **1** is defined here for the amount needed to create the (4 × 4) overlayer on Cu(111) at room temperature,¹⁵ i.e., 9×10^{17} molecule/m².

Theoretical. The conformational analyses of the molecular systems were carried out using the B97D/Def2-TZVPP level of theory.³² The semiempirically corrected functional, B97D, is in accord to the ansatz proposed by Grimme (2006),^{33,34} using an ultrafine grid for evaluation of integrals. The B97-D functional is a special reparameterization of the original B97 hybrid functional of Becke,³⁵ which is more neutral to spurious dispersion contamination in the exchange part than the original functional. The Def2-TZVPP basis set is that of Weigend and Ahlrichs.³⁶ Full geometry optimizations were performed and uniquely characterized via second derivatives (Hessian). From the fully optimized structures of the alkali-metal-**1** complexes, projected density of states (PDOS) were determined using the Perdew–Burke–Ernzerhof generalized gradient approximation (PBE-GGA),³⁷ plane wave basis sets, and Vanderbilt ultrasoft pseudopotentials,³⁸ implemented in the Quantum-ESPRESSO package.³⁹ The dimensions of the unit cell are such that the distance among replicas are on the order of 20 Å. Rydberg cut-offs of 25 and 250 are chosen for the wave functions and the charge density, respectively. The calculations are performed at the GAMMA point.

RESULTS AND DISCUSSION

Figure 2 displays a series of UP spectra of a thick film of metallic Cs with increasing coverage of **1** at 100 K sample temperature. The spectrum of the metallic Cs film (black curve) features the characteristic 5p_{1/2} and 5p_{3/2} peaks of cesium at 12 and 13.8 eV binding energy as well as the characteristic valence Auger edge at 9.5 eV. The Cs film is thick enough to extinct any Cu feature. The 5p_{1/2} peak is split into a very sharp doublet, which occurs as the valence auger edge only in metallic Cs films. The weak emission of electrons from the Fermi edge is also clearly identified (Figure 2, inset). The 5p peaks disappear upon gradual deposition of **1** and are completely quenched in the 3 ML spectrum; an indication of layer-by-layer growth, because otherwise features of the underlying Cs film would be still observed. For initial coverages of **1** (up to ~1 ML), two new features (A' and A'') appear in the molecular band gap at 0.8 and 2.6 eV binding energy,

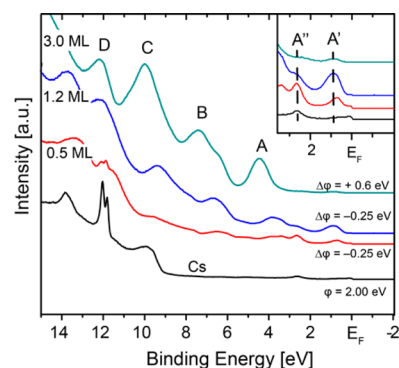


Figure 2. UP spectra of a clean Cs film (black) subsequently covered with one-half (red), 1.2 (blue), and three (green) monolayers of **1**. The inset shows emergence of new occupied states (A') near the Fermi edge. $T = 100$ K. Values of the work function of metallic Cs and work function change due to deposition of **1** are given.

respectively. These new peaks are associated with the corannulene LUMOs becoming occupied by formation of a charge-transfer complex with the underlying Cs. The work function of 2.0 eV of metallic Cs, as determined from the secondary electron cutoff here (not shown), is in good agreement with previously reported values in the literature.⁴⁰ The work function of the Cs doped film of **1** is even lower at 1.75 eV. The spectrum taken with 3 ML COR refers to the undoped multilayer of corannulene, as can be seen in the increased work function and the disappearance of the gap states, again indicating a layer-by-layer growth of the molecular film and no diffusion of the alkali metal. The bands of **1** (A–D) are also observed for deposition on Cu(111) without Cs involved.⁴¹

Multilayers of **1** desorb between 300 and 330 K and multilayered metallic Cs desorbs also at 300 K.⁴¹ Heating a thick (≈ 10 ML) film of **1** adsorbed on the thick Cs film, both deposited at 100 K, does not result in such multilayer desorption of components but rather in the formation of a compound surface coating with thermal stability beyond those of the single components.

Figure 3 shows the UP spectra with increasing temperatures. The spectra at higher temperature show that the multilayer bands of the single components (Figure 2) disappeared. Furthermore, Cu bands are not observed, confirming that we still deal with a thick film. Between 200 and 300 K, the spectra change drastically. On one hand the molecular features (A–D) decrease in intensity, broaden, and show initially a rigid shift to higher binding energy. On the other hand the now-occupied LUMOs (A' and A'') and a second peak, associated with the destabilized HOMO, appear. Upon heating to 420 K the Cs-doped **1** A' and A'' emissions are still very pronounced and show no sign of decomposition. Starting from 275 K the LUMOs are clearly visible around 1.0 and 2.5 eV. At increased temperatures the Cs becomes mobile and diffuses into the film resulting in a change in the local density of Cs atoms per molecule.

Between 275 and 300 K, band A (presenting two degenerate HOMOs) broadens and shifts to slightly lower binding energy, whereas the gap states A' and A'' shift to slightly higher binding energy, thus decreasing the former HOMO–LUMO gap. This observation and the growing intensity of the LUMOs must be interpreted as the Cs increasingly dispersing in the film of **1** above and doping all the molecular layers that were undoped in

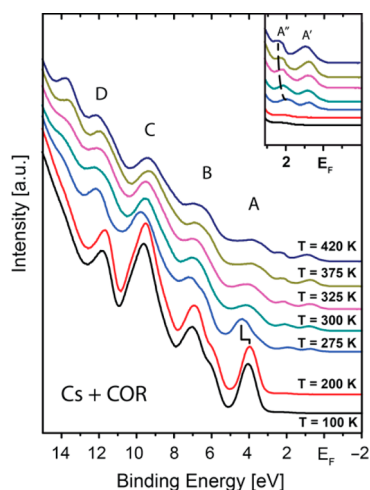


Figure 3. Evolution of valence band spectra with temperature of a 10 ML sample of **1** on top a thick Cs film on Cu(111). The inset shows emergence of new occupied states (A' and A'') just below the Fermi edge with increasing temperature due to occupation of the degenerate LUMOs.

the thick film before. Similar conclusions have been made for potassium doping of C_{60} multilayers.^{42,43} Moreover, there is no sign of increased intensity around the Cu d-band or the Fermi level indicating that desorption is not an issue and decomposition negligible, as indicated by the intact molecular structure. During this annealing procedure, the work function decreases from 3.4 eV at 100 K to 2.0 eV at 420 K, an indication that the diffusion of Cs and **1** still prevails. The gradual intensity increase of the two A' and A'' photoelectron emission peaks supports this picture.

The appearance of two new gap states below the Fermi edge in the valence band UP spectra indicates that the two degenerate LUMOs become populated, but not if they are completely or only partially filled. As mentioned above, with Li, a tetraanion has been reported.²⁴ Because Cs has a much lower ionization potential, such charge transfer can be expected from this point of view; however, the maximum reduction to -2 with potassium has been assigned to steric issues. Our XPS analysis of the film after thermal treatment (Figure 4), which is based

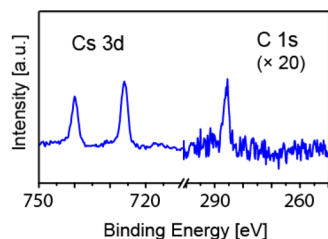


Figure 4. XP spectra of the Cs 3d and C 1s peak regions of a thick annealed Cs-**1** film. From the peak areas results a carbon:cesium ratio of 5.1:1.

on the intensity of the Cs $3d_{5/2}$ and C 1s peaks in the spectrum plus taking the corresponding sensitivity factors into account, reveals a carbon:cesium ratio of 5.1:1, i.e., basically four Cs atoms per one molecule of **1**. This supports the proposed tetraanionic corannulene and the full occupation of the two degenerate LUMO and LUMO+1. A calculation of the PDOS and the symmetry structure of the highest occupied orbitals of the complex, which are identical to the LUMO of the free

molecule, further supports the four-fold occupation of LUMO and LUMO+1 (Figure S1).

In order to evaluate the structure of complex of **1** and Cs in the film, we performed modeling at the B97D/Def2-TZVPP level of theory for different structures. Cs-corannulene complexes, including Cs_4 -**1** monomer structures and $(Cs_4-1)_2$ dimer structures, have been fully optimized. Two monomer structures were optimized, one with two Cs atoms approaching the convex side and two Cs atoms approaching the concave side of **1** and one with all 4 Cs atoms approaching the convex side of **1** (Figure S2). The latter was calculated to be higher in energy (21 kcal/mol); however, a much more stable situation was found for the fully optimized dimer complex resulting in a stacked conformation, with four Cs atoms coordinated between the two stacked corannulene molecules and two Cs atoms on the outer face of each bowl (Figures 5 and S2). An estimate of the complexation energy for the dimer, with reference to the lowest energy monomer structure, predicted a significant stabilization of the dimer by ~ 156 kcal/mol. Such large stabilization energy may be in part due to the increased interaction capability of the Cs atoms between the two structures, which bind to both of the corannulene surfaces (Figure 5).

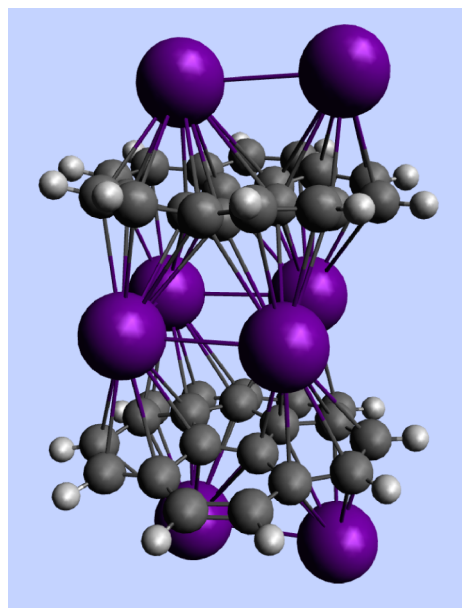


Figure 5. B97D/Def2-TZVPP optimized structure of the $Cs_8C_{20}H_{10}$ complex.

CONCLUSIONS

The interaction of Cs leads to a quadruple anion of corannulene in the solid state. In contrast to earlier claims, four Cs atoms are found to be located between two bowls in a sandwiched structure. Valence band spectra show population of two electronic levels that are assigned as the two degenerate LUMO orbitals of corannulene. Up to 420 K, no decomposition was observed. Having a method for preparing films of X-**1** at maximum alkali-metal doping level opens the door to study superconductivity and optoelectronic properties of these promising materials systems.

■ ASSOCIATED CONTENT

S Supporting Information

DOS, PDOS, highest occupied orbitals of Cs-1 complex, and DFT-optimized complex structures. This material is available free of charge via the Internet at <http://pubs.acs.org>.

■ AUTHOR INFORMATION

Corresponding Author

karl-heinz.ernst@empa.ch; kimb@oci.uzh.ch

Notes

The authors declare no competing financial interest.

■ ACKNOWLEDGMENTS

Financial support from the Swiss National Science Foundation (SNSF) and the Sino Swiss Science and Technology Cooperation (SSSTC) is gratefully acknowledged. We thank UZH-UFSP LightChEC for financial support. This work has been financially supported by the Austrian Science Fund (FWF) via project P21330-N20.

■ REFERENCES

- (1) Ishiguro, T.; Yamaji, K.; Saito, G. *Organic Superconductors*, 2nd ed.; Springer: Berlin, 1998.
- (2) Hannay, N. B.; Geballe, T. H.; Matthias, B. T.; Andres, K.; Schmidt, P.; MacNair, D. *Phys. Rev. Lett.* **1965**, *14*, 225–226.
- (3) Emery, N.; Hérol, C.; d'Astuto, M.; Garcia, V.; Bellin, C.; Maréché, J. F.; Lagrange, P.; Loupiau, G. *Phys. Rev. Lett.* **2005**, *95*, 087003/1–4.
- (4) Weller, T. E.; Ellerby, M.; Saxena, S. S.; Smith, R. P.; Skipper, N. T. *Nat. Phys.* **2005**, *1*, 39–41.
- (5) Rosseinsky, M. J.; Ramirez, A. P.; Glarum, S. H.; Murphy, D. W.; Haddon, R. C.; Hebard, A. F.; Palstra, T. T. M.; Kortan, A. R.; Zahurak, S. M.; Makhija, A. V. *Phys. Rev. Lett.* **1991**, *66*, 2830–2832.
- (6) Ganin, A. Y.; Takabayashi, Y.; Khimiyak, Y. Z.; Margadonna, S.; Tamai, A.; Rosseinsky, M. J.; Prassides, K. *Nat. Mater.* **2008**, *7*, 367–371.
- (7) Mitsuhashi, R.; Suzuki, Y.; Yamanari, Y.; Mitamura, H.; Kambe, T.; Ikeda, N.; Okamoto, H.; Fujiwara, A.; Yamaji, M.; Kawasaki, N.; Maniwa, Y.; Kubozono, Y. *Nature* **2010**, *464*, 76–79.
- (8) Xue, M.; Chen, G.; Yang, H.; Zhu, Y.; Wang, D.; He, J.; Cao, T. J. *Am. Chem. Soc.* **2013**, *134*, 6536–6539.
- (9) Kato, T.; Yamabe, T. *J. Chem. Phys.* **2002**, *117*, 2324–2331.
- (10) Bauert, T.; Merz, L.; Bandera, D.; Parschau, M.; Siegel, J. S.; Ernst, K.-H. *J. Am. Chem. Soc.* **2009**, *131*, 3460–3461.
- (11) Zoppi, L.; Bauert, T.; Siegel, J. S.; Baldrige, K. K.; Ernst, K.-H. *Phys. Chem. Chem. Phys.* **2012**, *14*, 13365–13369.
- (12) Parschau, M.; Fasel, R.; Ernst, K.-H.; Gröning, O.; Brandenberger, L.; Schillinger, R.; Greber, T.; Seitsonen, A.; Wu, Y.-T.; Siegel, J. S. *Angew. Chem., Int. Ed.* **2007**, *46*, 8258–8261.
- (13) Angelova, P.; Solel, E.; Parvi, G.; Turchanin, A.; Botoshansky, M.; Götzhäuser, A.; Keinan, E. *Langmuir* **2013**, *29*, 2217–2233.
- (14) Guillermet, O.; Niemi, E.; Nagarajan, S.; Bouju, X.; Martrou, D.; Gourdon, A.; Gauthier, S. *Angew. Chem., Int. Ed.* **2009**, *48*, 1970–1973.
- (15) Merz, L.; Parschau, M.; Zoppi, L.; Baldrige, K. K.; Siegel, J. S.; Ernst, K.-H. *Angew. Chem., Int. Ed.* **2009**, *48*, 1966–1969.
- (16) Merz, L.; Bauert, T.; Parschau, M.; Koller, G.; Siegel, J. S.; Ernst, K.-H. *Chem. Commun.* **2009**, 5871–5873.
- (17) Calmettes, B.; Nagarajan, S.; Gourdon, A.; Abel, M.; Porte L. Coratger, R. *Angew. Chem., Int. Ed.* **2008**, *47*, 6994–6998.
- (18) Xiao, W.; Passerone, D.; Ruffieux, P.; Ait-Mansour, K.; Gröning, O.; Tosatti, E.; Siegel, J. S.; Fasel, R. *J. Am. Chem. Soc.* **2008**, *130*, 4767–4771.
- (19) Bauert, T.; Baldrige, K. K.; Siegel, J. S.; Ernst, K.-H. *Chem. Commun.* **2011**, *47*, 7995–7997.
- (20) Wu, Y.-T.; Siegel, J. S. *Chem. Rev.* **2006**, *106*, 4843–4867.
- (21) Tsefrikas, V. M.; Scott, L. T. *Chem. Rev.* **2006**, *106*, 4868–4884.
- (22) Wu, Y.-T.; Bandera, D.; Maag, R.; Linden, A.; Baldrige, K. K.; Siegel, J. S. *J. Am. Chem. Soc.* **2008**, *130*, 10729–10739.
- (23) Valenti, G.; Bruno, C.; Rapino, S.; Fiorani, A.; Jackson, E. A.; Scott, L. T.; Paolucci, F.; Marcaccio, M. *J. Phys. Chem. C* **2010**, *114*, 19467–19472.
- (24) Aprahamian, I.; Eisenberg, D.; Hoffman, R. E.; Sternfeld, T.; Matsuo, Y.; Jackson, E. A.; Nakamura, E.; Scott, L. T.; Sheradsky, T.; Rabinovitz, M. *J. Am. Chem. Soc.* **2005**, *127*, 9581–9587.
- (25) Ayalon, A.; Sygula, A.; Cheng, P.-C.; Rabinovitz, M.; Rabideau, P. W.; Scott, L. T. *Science* **1994**, *265*, 1065–1067.
- (26) Baumgarten, M.; Gherghel, J. L.; Wagner, M.; Weitz, A.; Rabinovitz, M.; Cheng, P.-C.; Scott, L. T. *J. Am. Chem. Soc.* **1995**, *117*, 6254–6257.
- (27) A claim made in: Aprahamian, I.; Preda, D. V.; Bancu, M.; Belanger, A.; Sheradsky, T.; Scott, L. T.; Rabinovitz, M. *J. Org. Chem.* **2006**, *71*, 290–298 with reference to a Ph.D. thesis written in Hebrew. We are therefore not able to verify the bases of this conclusion.
- (28) Spisak, S. N.; Zabula, A. V.; Filatov, A. S.; Rogachev, A. Y.; Petrukhina, M. A. *Angew. Chem., Int. Ed.* **2011**, *50*, 8090–8094.
- (29) Zabula, A. V.; Filatov, A. S.; Spisak, S. N.; Rogachev, A. Y.; Petrukhina, M. A. *Science* **2011**, *333*, 1008–1011.
- (30) Eisenberg, D.; Quimby, J. M.; Jackson, E. A.; Scott, L. T.; Shenhar, R. *Chem. Commun.* **2010**, *46*, 9010–9012.
- (31) Ernst, K.-H.; Kuster, Y.; Fasel, R.; Müller, M.; Ellerbeck, U. *Chirality* **2001**, *13*, 675–678.
- (32) Schmidt, M.; Baldrige, K. K.; Boatz, J. A.; Elbert, S.; Gordon, M.; Jenson, J. H.; Koeski, S.; Matsunaga, N.; Nguyen, K. A.; Su, S. J.; Windus, T. L.; Dupuis, M.; Montgomery, J. A. *J. Comput. Chem.* **1993**, *14*, 1347–1363.
- (33) Grimme, S. *J. Comput. Chem.* **2006**, *27*, 1787–1799.
- (34) Peverati, R.; Baldrige, K. K. *J. Chem. Theory Comput.* **2008**, *4*, 2030–2048.
- (35) Becke, A. D. *Phys. Rev. A* **1988**, *38*, 3098–3100.
- (36) Weigend, F.; Ahlrichs, R. *Phys. Chem. Chem. Phys.* **2005**, *7*, 3297–3305.
- (37) Perdew, J. P.; Burke, K.; Ernzerhof, M. *Phys. Rev. Lett.* **1996**, *77*, 3865–3868.
- (38) Vanderbilt, D. *Phys. Rev. B* **1990**, *41*, 7892–7895.
- (39) Giannozzi, P.; Baroni, S.; Bonini, N.; Calandra, M.; Car, R.; Cavazzoni, C.; Ceresoli, D.; Chiarotti, G. L.; Cococcioni, M.; Dabo, I.; Dal Corso, A.; de Gironcoli, S.; Fabris, S.; Fratesi, G.; Gebauer, R.; Gerstmann, U.; Gougoussis, C.; Kokalj, A.; Lazzeri, M.; Martin-Samos, L.; Marzari, N.; Mauri, F.; Mazzarello, R.; Paolini, S.; Pasquarello, A.; Paulatto, L.; Sbraccia, C.; Scandolo, S.; Sclauzero, G.; Seitsonen, A. P.; Smogunov, A.; Umari, P.; Wentzcovitch, R. M. *J. Phys.: Condens. Matter* **2009**, *21*, 395502/1–19.
- (40) Stolz, H.; Höfer, M.; Wassmuth, H.-W. *Surf. Sci.* **1993**, *287/288*, 564–567.
- (41) Bauert, T.; Zoppi, L.; Koller, G.; Garcia, A.; Baldrige, K. K.; Ernst, K.-H. *J. Phys. Chem. Lett.* **2011**, *2*, 2805–2809.
- (42) Hoogenboom, B. W.; Hesper, R.; Tjeng, L. H.; Sawatzky, G. A. *Phys. Rev. B* **1998**, *57*, 11939–11942.
- (43) Cepek, C.; Sancrotti, M.; Greber, T.; Osterwalder, J. *Surf. Sci.* **2000**, *454–456*, 467–471.